A Configurable 5.9 μW Analog Front-End for Biosignal Acquisition

Tan Yang[1], Junjie Lu[2], M. Shahriar Jahan[1], Kelly Griffin[1], Jeremy Langford[1], and Jeremy Holleman[1]

[1]Department of EECS, University of Tennessee, Knoxville, TN 37996, USA

[2]Broadcom Corporation, Irvine, CA, USA

***Abstract* — This paper presents a configurable analog front-end (AFE) for the recordings of a variety of biopotential signals, including electromyography (EMG), electrocardiogram (ECG), electroencephalogram (EEG), action potential (AP) signals, etc. The first stage of the AFE employs a chopper-stabilized current-reuse complementary input (CRCI) telescopic-cascode amplifier to achieve high noise-power efficiency and suppress 1/*f* noise. A tunable impedance-boosting loop (IBL) is utilized, which is robust to process variation and parasitic capacitance and increases the input impedance from 4.3 MΩ to 102 MΩ. The proposed AFE is fabricated in a 0.13 μm CMOS process. The AFE has a mid-band gain from 45.2-71 dB. The low-pass corner is tunable in the range of 70-400 Hz and 1.2-7 kHz. When configured for EEG recordings (0.7-100 Hz), the AFE draws 5.4 μW from a 1.2 V supply while exhibiting input-referred noise of 0.45 μVrms, corresponding to a noise efficiency factor (NEF) of 3.7. When configured for AP recordings (0.7 Hz-7 kHz), the AFE consumes 5.9 μW with input referred noise of 2.93 μVrms and a NEF of 3.0.**

***Index Terms* — Current-reuse complimentary input (CRCI), chopper stabilized, configurable, analog front-end (AFE), biosignal acquisition.**

I. Introduction

Biopotential signals (EEG, ECG, EMG, AP, etc.) provide vital information about the patients which allow clinicians to diagnose and treat diseases like muscle paralysis, cardiovascular diseases, brain injuries, epilepsy, etc. Biopotential signals have different frequency and amplitude characteristics. For example, EEG signals have amplitudes from 1 μV to 100 μV with much of the energy in the sub-Hz to 100 Hz band. AP signals have amplitudes up to 500 μV with much of the energy in the 100 Hz to 7 kHz band. In order to improve the quality of healthcare, it is desirable to have a biosignal acquisition system suitable for a variety of biopotential signals. In such a system, a configurable low-noise AFE is required. Besides, in wearable/implantable systems, low-power operation is essential to extend battery life and avoid thermal damage to surrounding tissues.

Several recent efforts have advanced the state-of-the-art of low-power low-noise biopotential amplifiers [1]-[5]. Amplifiers in [1], [2] achieved good low-frequency noise (<1 μV_{rms}) by using capacitively coupled chopper topology, but focused only on NFP/EEG (sub-Hz to 100 Hz) acquisition. Dual-band AFEs in [3]-[5] were designed for local field potentials (LFPs, <200 Hz) and AP acquisition. However, the designs in [3], [4] exhibited inferior low-frequency noise (4.3 μV_{rms} and 14 μV_{rms}, respectively). The design reported in [5] employed a DC-coupled source-degenerated topology to achieve high input impedance, while sacrificing power efficiency which resulted in an inferior NEF of 7.6.

In this paper, we present a power-efficient AFE with configurable bandwidth and gain. The AFE employs a chopper-stabilized current-reuse complementary input (CRCI) telescopic-cascode amplifier to achieve high noise-power efficiency and suppress the low-frequency noise. A tunable input impedance-boosting loop (IBL) compensates for process variation and parasitic capacitance, and maximizes the input impedance-boosting factor. The AFE's performance is demonstrated with biological measurements.

II. Analog Front End Design

Fig. 1 shows the configuration of the proposed AFE. The AFE comprises a first-stage chopper-stabilized low-noise amplifier (LNA), a second-stage variable-gain amplifier (VGA), a tunable high-linearity 2nd-order low-pass filter (LPF), and two single-ended third-stage amplifiers. The gain of the AFE ranges from 46 dB to 72 dB. The 2nd-order LPF is used to tune cut-off frequency, and filter out the up-modulated low-frequency noise and the chopping ripple. The third stage provides additional gain of 6 dB. The LPF is placed between the VGA and the third stage to relax its noise and linearity requirement. A fully differential architecture is employed to provide high common-mode rejection ratio (CMRR) and power-supply rejection ratio (PSRR).

A. First-Stage LNA Design

The LNA employs capacitive feedback to set mid-band gain (C_{in1}/C_{fb1}). Chopper modulation (f_c = 25 kHz) is used to suppress low-frequency noise. The input impedance is limited by the equivalent switched-capacitor impedance formed by *CH*1 and C_{in1}. A capacitive input impedance boosting loop (IBL) [7] exploits partial positive feedback to increase the input impedance without extra current consumption. In order to compensate for the process

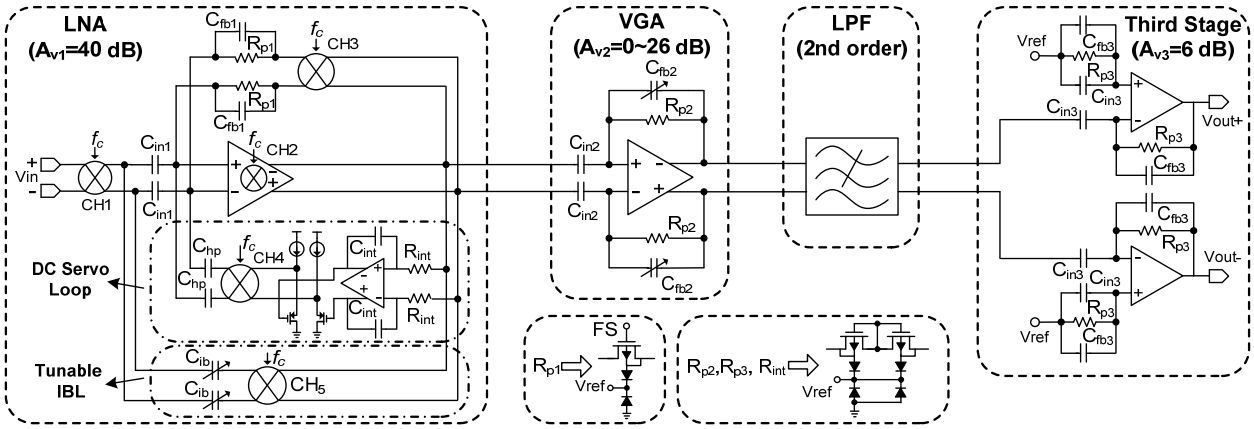

Fig.1. Configuration of the proposed AFE.

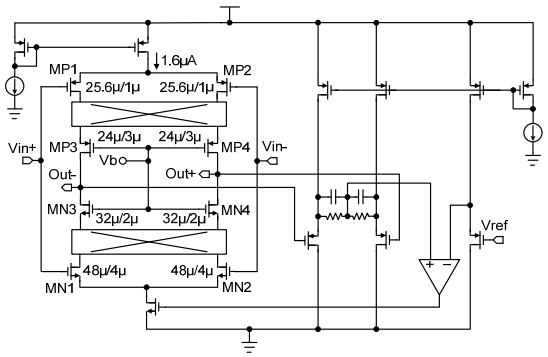

Fig.2. Schematic of the chopper-stabilized CRCI telescopic-cascode amplifier.

variation and capacitance associated with C_{in1}'s bottom plate and achieve maximum impedance boosting factor, tunable capacitors (C_{ib}) are used in our design. The DC servo loop defines the high-pass cutoff characteristics of the amplifier to reject large DC electrode offsets. PMOS source-followers act as buffers for the integrator to drive the switched-capacitor load. The triple-well NMOS transistors (R_{p1}) are normally biased in subthreshold region to set DC bias, and they can also act as reset switches.

A highly power-efficient single-ended amplifier based on current-reuse complementary input (CRCI) technique was reported in [7]. By driving the gates of both PMOS and NMOS input transistors, the CRCI technique fully reuses the current and doubles the effective transconductance, which leads to a significant reduction in input-referred noise. Compared with the folded-cascode OTA, telescopic-cascode OTA which has fewer current branches, is more power efficient. The LNA employs the chopper-stabilized CRCI telescopic-cascode OTA, which is shown in Fig. 2. The gates of the N- and P-type cascode devices are tied together to save one bias reference and simplify the design. Chopper modulators are placed at the low-impedance node at the sources of the cascode transistors [1], which allows chopping the amplifier at higher frequencies. To further improve the noise-power efficiency, the complementary-input transistors (*MP*1,2 and *MN*1,2) are biased in weak inversion to maximize their g_m/I_D ratio, and the cascode transistors (*MP*3,4 and *MN*3,4) use large size to minimize their *1/f* noise, because their *1/f* noise is not up-modulated.

The input-referred thermal noise of the CRCI telescopic-cascode OTA can be approximated as:

$$V_{ni,OTA}^2 = \frac{4kT}{\kappa(g_{mn1} + g_{mp1})} \cdot \Delta f \qquad (1)$$

where g_{mp1} and g_{mn1} represent the transconductance of input PMOS (*MP*1,2) and NMOS (*MN*1,2), respectively, and κ is the reciprocal of the sub-threshold slope factor n_p.

B. Second-Stage VGA Design

The VGA uses a tunable capacitor bank to set the mid-band gain from 0 dB-26 dB in a step of no larger than 3 dB. Pseudo-resistors are employed to obtain a sub-Hz high-pass cutoff. A folded-cascode OTA is used to provide adequate open-loop gain and output swing. The transistors are carefully sized to minimize their noise contribution.

C. 2nd-order LPF Design

A tunable high-linearity transconductor cell based on transistors biased in the triode region in a BiCMOS process was reported in [8]. Fig. 3(a) shows the transconductor cell modified for CMOS. *MP*1/*MP*2 are the input transistors biased in triode region by the cascode transistors *MP*3/*MP*4. V_{tune} determines V_{DS} of the input transistors and therefore the G_m of the transconductor. Transistors *MP*3/*MP*4 are biased in deep weak inversion to significantly reduce V_{DS} variation so that it does not degrade linearity. The common-mode feedback (CMFB) circuit uses a structure similar to the differential-mode (DM) path and therefore offers comparable linearity. The

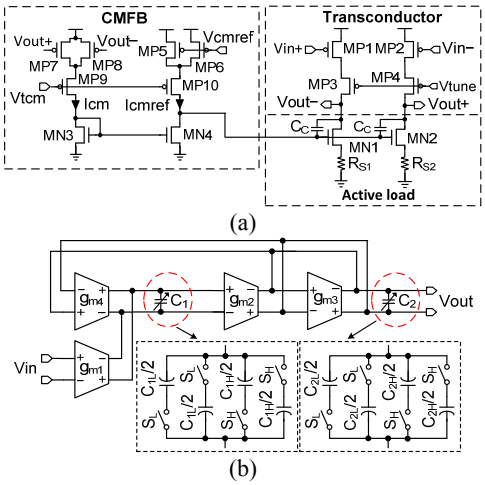

Fig. 3. (a) Schematic of the linear transconductor cell. (b) 2nd-order LPF structure.

noise is optimized by properly sizing the transistors and using source degeneration.

The configuration of a second-order Butterworth LPF adopting the Biquad structure is shown in Fig. 3(b). We choose $g_{m1\text{-}4} = g_m$ to facilitate matching. Transconductors g_{m1} and g_{m4} share the same output nodes, as do g_{m2} and g_{m3}. Therefore, each pair can share their cascode transistors, active loads and CMFB circuits, significantly reducing the area and power consumption of the filter system. Adjustable capacitors C_1 and C_2 combined with the tunable transconductor set the low-pass cutoff from 70-400 Hz and from 1.2-7 kHz.

D. Third-Stage Amplifier Design

The gain of the third stage is set to be 6 dB by capacitive feedback. A current-mirror OTA is employed to achieve wide output swing.

III. Measurement Results

The AFE is fabricated in a 0.13 µm CMOS process. The die microphotograph is shown in Fig. 4. The active area is 400 µm × 1000 µm. The AFE draws 4.4-4.9 µA from a 1.2 V supply. Fig. 5(a) shows the measured transfer function of the AFE. The high-pass cutoff is around 0.7 Hz. The low-pass cutoff is tunable in the range of 70-400 Hz and 1.2-7 kHz. The input-referred noise the proposed AFE is shown in Fig. 5(b). The thermal noise density is 34 nV/sqrt(Hz). The flicker noise corner is down to 25 Hz by using chopper technique. When the AFE is configured for AP recordings (0.7 Hz-7 kHz), the input-referred noise is 2.93 µVrms integrated from 1 Hz to 50 kHz, corresponding to a NEF of 3.0. When configured for EEG recordings (0.7-100 Hz), the input-referred noise is 0.45 µVrms, corresponding to a NEF of 3.7.

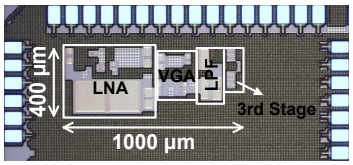

Fig. 4. Die microphotograph of the proposed AFE.

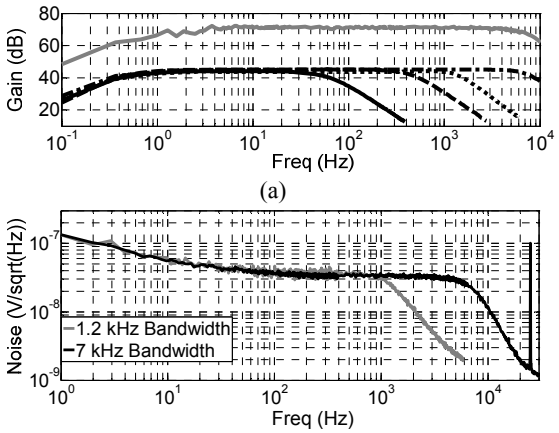

Fig. 5. (a) Measured transfer function. (b) Measured input-referred noise at the gain of 66 dB.

The proposed AFE is compared with previous work in Table I. To facilitate comparison, we use the noise efficiency factor (NEF) [9] and the power efficiency factor (PEF) [3], which are widely utilized as the figure-of-merit to evaluate biopotential AFEs. Compared with other benchmarks, the proposed AFE exhibits the lowest noise in EEG band (1-100 Hz). It achieves the best NEF and PEF in EEG band compared with other benchmarks, which indicates the highest noise-power efficiency in EEG band. The linearity of the proposed AFE is worse than the AFEs in [1] and [5]. This is partly due to the lower supply voltage we use.

To demonstrate the performance, the AFE is used to obtain the recordings of several biopotential signals. Fig. 6(a) and (b) shows recorded human ECG signals and human EMG signals during repeated arm extensions, respectively. Fig. 6(c) shows the normalized spectrum of the measured EEG during eyes open and eyes closed. The dry electrodes are placed in positions of O1 and Cz of the head using the international 10-20 electrode placement system. Alpha waves (8-12 Hz) are clearly visible when the subject's eyes are closed and mentally relaxed, and are suppressed when eyes are open.

IV. Conclusion

A configurable AFE is presented, which is suitable for a variety of biopotential signals. To achieve high noise-

Table I. PERFORMANCE COMPARISON

	[1]	[2]	[3]	[4]	[5]	This work
Supply (V)	1.8	1.8	0.5	1.2	3.3	**1.2**
Power (μW)	1.8*	8.25*	5.05	35	73.9*	**5.3-5.9**
Gain (dB)	41, 50.5	52-80	32	40, 56	46, 66	**45.2-71**
Noise (μV_{rms})	0.98 (.05-100 Hz)	0.91 (.5-100 Hz)	4.3 (300 Hz) 4.9 (10 kHz)	14 (1-100 Hz) 2.2 (280-10 kHz)	0.9 (1-200 Hz) 3.3 (200-10 kHz)	**0.45 (1-100 Hz) 2.93 (1 Hz-7 kHz)**
NEF	4.6	5.1	6.0	4.5 (280-10 kHz)	7.6	**3.7 (1-100 Hz) 3.0 (1 Hz-7 kHz)**
PEF ($NEF^2 \cdot VDD$)	38*	47 *	18	24* (280-10 kHz)	190*	**16.4 (1-100 Hz) 10.8 (1 Hz-7 kHz)**
Bandwidth (Hz)	0.05-100	0.5-100	300, 10k	sub-Hz to100, 280-10k	0.1-200, 200-10k	**f_H <1, f_L=70-400, 1.2k-7k**
Z_{in} (MΩ)	8	>500	$1000\|\|C_{in}$	—	100 (1-200 Hz) 320@1 kHz	**>100**
THD@1mV_{pp}	< 0.1%	—	>2%	—	< 0.1%	**<1%**
CMRR (dB)	>100	—	75	—	>110	**>95**
Area (mm^2)	1.7	—	0.013	0.26	0.15	**0.4**
Process (μm)	0.8	0.18	0.065	0.13	0.35	**0.13**

*The value is calculated based on the reported performance.

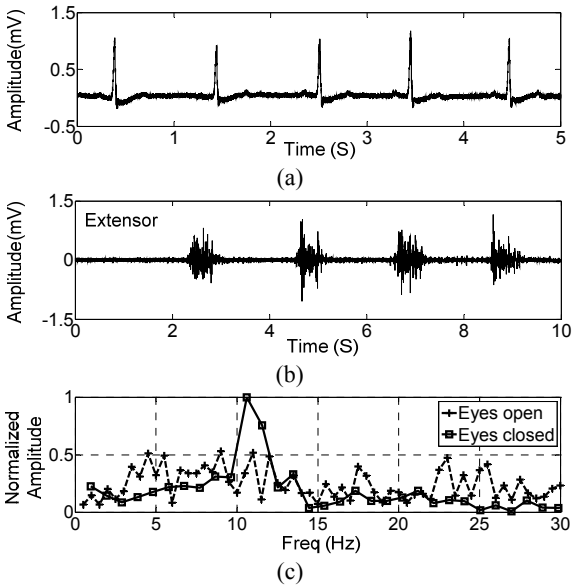

Fig. 6. (a) Human ECG recordings. (b) Human EMG recordings. (c) Human EEG recordings during eyes open and eyes close.

power efficiency, a chopper-stabilized LNA based on CRCI telescopic-cascode OTA is proposed. The input impedance increases from 4.3 MΩ to 102 MΩ with the tunable IBL. The AFE achieves 0.45 μVrms of input-referred noise in EEG band (1-100 Hz) and 2.93 μVrms in AP band (1 Hz-7 kHz), with NEF of 3.7 and 3.0, respectively. Compared with other benchmarks, the proposed AFE is the most noise-power efficient in EEG band (1-100 Hz).

ACKNOWLEDGEMENT

This work was partially supported by the National Science Foundation under grant DBI-1152361.

REFERENCES

[1] T. Denison, K. Consoer, W. Santa, A. T. Avestruz, J. Cooley, and A. Kelly, "A 2 μW 100 nV/rtHz chopper-stablized instrumentation amplifier for chronic measurement of neural field potentials," *IEEE J. Solid-State Circuits.,* vol. 42, pp. 2934-2945, Dec 2007.

[2] J. Yoo, L. Yan, D. El-Damak, M. A. B. Altaf, A. H. Shoeb, and A. P. Chandrakasan, "An 8-channel scalable EEG acquisition SoC with patient-specific seizure classification and recording processor," *IEEE J. Solid-State Circuits.*, pp. 214-228, Jan 2013.

[3] R. Muller, S. Gambini, and J. Rabaey, "A 0.013 mm^2 5 μW dc-coupled neural signal acquisition IC with 0.5 V supply," *IEEE J. Solid-State Circuits*, vol. 47, pp. 232-243, Jan 2012.

[4] H. Gao, R. M. Walker, P. Nuyujukian, K. A. A. Makinwa, K. V. Shenoy, B. Murmann, and T. H. Meng, "HermesE: a 96-channel full data rate direct neural interface in 0.13 μm CMOS," *IEEE J. Solid-State Circuits.*, pp. 1043-1055, April 2012.

[5] J. Guo, J. Yuan, J. Huang, J. K. Law, C. Yeung, and M. Chan, "32.9 nV/rt Hz -60.6 dB THD dual-band micro-electrode array signal acquisition IC," *IEEE J. Solid-State Circuits.*, pp. 1209-1220, May 2012.

[6] Q. Fan, F. Sebastiano, J. H. Huijsing, and K. A. A. Makinwa, "A 1.8 μW 60 nV/rtHz capacitively-coupled chopper instrumentation amplifier in 65 nm CMOS for wireless sensor nodes," *IEEE J. Solid-State Circuits.,* vol. 46, pp. 1534-1543, Jul 2011.

[7] J. Holleman, and B. Otis, "A sub-microwatt low-noise amplifier for neural recording," in *Proc. 29th Annu. Int. Conf. IEEE Engineering in Medicine and Biology Society*, 2007.

[8] J. Lu, T. Yang, M.S. Jahan, and J. Holleman, "A low-power 84-dB dynamic-range tunable Gm-C filter for bio-signal acquisition," in *Proc. IEEE Int. Midwest Symp. Circuits and Syst. (MWCAS),* pp. 1029-1032, Aug 2014.

[9] M. S. J. Steyaert, W. M. C. Sansen, and Z. Chang, "A micropower low-noise monolithic instrumentation amplifier for medical purposes," *IEEE J. Solid-State Circuits*, vol. SC-22, pp. 1163-1168, Dec. 1987.